Critical Froude number for transition from a steady to an unsteady fountain injected into a homogeneous fluid

N. Srinarayana[1], S. W. Armfield[1], M. Behnia[1] and Wenxian Lin[2]

[1]School of Aerospace, Mechanical and Mechatronic Engineering,
The University of Sydney, NSW 2006, Australia

[2]School of Engineering and Physical Sciences,
James Cook University, Townsville, QLD 4811, Australia

Abstract

In this paper, we present the critical Froude number for unsteadiness at full development of plane fountains. Numerical investigations are conducted over the range of Reynolds number, $6 \leq Re \leq 120$. The critical Froude number for transition from a steady to unsteady flow varies with the Reynolds number. For $Re \gtrsim 60$, the transition is independent of Re and is nearly constant at a Froude number of $Fr \sim 1.0$. Over the range $6 < Re \lesssim 50$, there is a significant increase in the transition Froude number.

Introduction

A fountain, also known as a negatively buoyant jet, is formed whenever a fluid is injected upwards into a lighter fluid, or downward into a denser fluid. In both cases, buoyancy opposes the momentum of the ejected flow until the jet penetrates a finite distance and falls back towards the source.

The behavior of plane fountains is governed by the Reynolds, Froude, and Prandtl numbers, defined as,

$$
\begin{aligned}
Re &\equiv \frac{V_{in} X_{in}}{\nu}, \\
Fr &\equiv \frac{V_{in}}{\sqrt{g(\rho_{in} - \rho_\infty)/\rho_\infty X_{in}}} \\
&\equiv \frac{V_{in}}{\sqrt{g\beta(T_\infty - T_{in})X_{in}}}, \\
Pr &\equiv \frac{\nu}{\kappa},
\end{aligned}
\tag{1}
$$

where X_{in} and V_{in} are the half-width and average velocity at the fountain source respectively, ν is the kinematic viscosity of the fountain fluid, g is the acceleration due to gravity, ρ_{in} and T_{in} are the density and temperature of the fountain fluid at the source, ρ_∞ and T_∞ are the density and temperature of the ambient fluid, κ is the thermal diffusivity, and β is the coefficient of volumetric expansion, respectively. The second expression of the Froude number in equation (1) applies when the density difference is due to the difference in temperature of the fountain and ambient fluid using the Oberbeck–Boussinesq approximation. A schematic of a typical fountain is shown in figure 1, where a lighter fluid is injected upwards into denser fluid. The fountain after attaining a maximum height flow downward and along the floor and settles at a lesser penetration height of Z_m.

The first ever work on fountains began with Morton [1] who obtained analytical solution for the fountain penetration height. This work was later extended by Campbell and Turner [2] and Baines *et al.* [3], who conducted experiments on both round and planar fountains. In addition to experimental studies there have been some numerical studies by Lin and Armfield [4, 5], who investigated the effect
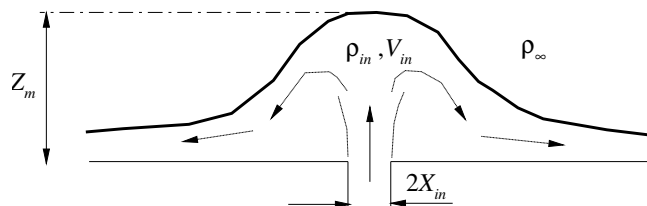

Figure 1: Schematic of a fountain.

of the Reynolds number on the height of planar fountains over the $0.2 \leq Fr \leq 1.0$ and $Re \leq 200$. Recently, Srinarayana *et al.* [6] obtained numerically the critical Froude number for unsteadiness in the fountain flow with a uniform velocity profile at the inlet as $Fr = 2.25$.

There are also investigations on the behavior of fountain flows, such as the stability, unsteadiness, transition, etc. Williamson *et al.* [7] conducted extensive experimental studies on low-Reynolds number round fountain behaviors. Srinarayana *et al.* [8] studied different flow regimes and instability modes for low Re plane fountains. There is, however, very little information on critical Froude number for unsteadiness of planar fountains and in this paper we present the same over the range $6 \leq Re \leq 120$.

Numerical model

The physical system considered here is a rectangular box filled with a fluid between the insulated top (ceiling) and bottom (floor) solid walls which are distance H apart. The fluid is initially still and isothermal at a temperature T_∞. The fountain source is a slot of width $2X_{in}$ in the center of the floor. For $t > 0$ the fluid issues from the slot with a temperature $T_{in} < T_\infty$ and a parabolic velocity profile

$$
V = V_m \left[1 - \left(\frac{X}{X_{in}} \right)^2 \right],
\tag{2}
$$

where V_m is the maximum velocity of the parabolic profile, equal to $1.5V_{in}$ for a fully developed laminar flow. The discharge conditions are maintained thereafter. The flow is assumed to remain two-dimensional. The computational domain is sketched in figure 2. The temperature difference between the source and ambient fluids results in the required buoyancy. The governing equations are the incompressible Navier–Stokes and energy equations with the Oberbeck–Boussinesq approximation. The following equations are written in conservative, non-dimensional form in Cartesian coordinates,
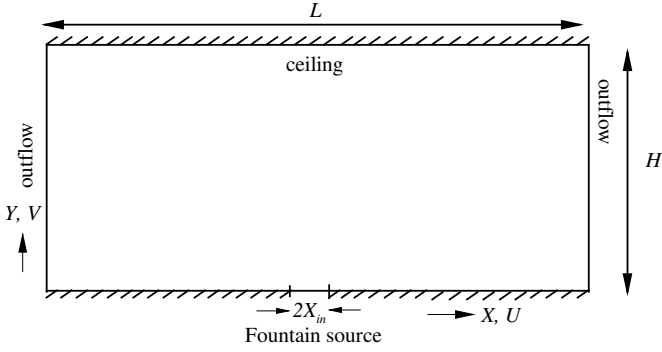
Figure 2: Computational domain.

$$\frac{\partial u}{\partial x} + \frac{\partial v}{\partial y} = 0, \tag{3}$$

$$\frac{\partial u}{\partial \tau} + \frac{\partial (uu)}{\partial x} + \frac{\partial (vu)}{\partial y} = -\frac{\partial p}{\partial x} + \frac{1}{Re}\left(\frac{\partial^2 u}{\partial x^2} + \frac{\partial^2 u}{\partial y^2}\right), \tag{4}$$

$$\frac{\partial v}{\partial \tau} + \frac{\partial (uv)}{\partial x} + \frac{\partial (vv)}{\partial y} = -\frac{\partial p}{\partial y} + \frac{1}{Re}\left(\frac{\partial^2 v}{\partial x^2} + \frac{\partial^2 v}{\partial y^2}\right) + \frac{1}{Fr^2}\theta, \tag{5}$$

$$\frac{\partial \theta}{\partial \tau} + \frac{\partial (u\theta)}{\partial x} + \frac{\partial (v\theta)}{\partial y} = \frac{1}{RePr}\left(\frac{\partial^2 \theta}{\partial x^2} + \frac{\partial^2 \theta}{\partial y^2}\right). \tag{6}$$

The following non-dimensionalisation is used:

$$x = \frac{X}{X_{in}}, y = \frac{Y}{X_{in}}, u = \frac{U}{V_{in}}, v = \frac{V}{V_{in}},$$

$$\tau = \frac{t}{(X_{in}/V_{in})}, p = \frac{P}{\rho V_{in}^2}, \theta = \frac{T - T_\infty}{T_\infty - T_{in}}. \tag{7}$$

The initial and boundary conditions are

$$u = v = \theta = 0 \text{ when } \tau < 0, \tag{8}$$

and when $\tau \geq 0$

$$\frac{\partial u}{\partial x} = 0, \frac{\partial v}{\partial x} = 0, \frac{\partial \theta}{\partial x} = 0 \text{ on } x = \pm L/(2X_{in}), \tag{9}$$

$$u = 0, v = 1.5(1 - x^2), \theta = -1 \text{ on } |x| \leq 1, y = 0, \tag{10}$$

$$u = v = 0, \frac{\partial \theta}{\partial y} = 0 \text{ on } |x| > 1, y = 0, \tag{11}$$

$$u = v = 0, \frac{\partial \theta}{\partial y} = 0 \text{ on } |x| \leq L/(2X_{in}), y = H/X_{in}, \tag{12}$$

respectively. The results are obtained using the open source code Gerris [9]. The computational domain is $-100 \leq x \leq +100$ and $0 \leq y \leq 100$.

Results

The results have been obtained for Reynolds numbers ranging from $6 \leq Re \leq 120$ and at a fixed Prandtl number of $Pr = 7$.

The difference between a steady and unsteady fountain at full development is demonstrated with time-evolution of fountains for $Fr = 1.17$ and $Fr = 1.2$ at $Re = 60$ and $Pr = 7$, shown in figure 3. After the fountain is initiated, it travels upwards until momentum balances buoyancy, when it comes to rest. The rising fluid spreads due to its reduced velocity and interaction with the ambient fluid. The descending fluid then interacts with the environment and with the upflow, restricting the rise of further fluid. The descending fluid, heavier than the ambient, moves along the floor as a gravity current. The fountain is symmetric and steady for $Fr = 1.17$ at full development whereas the fountain starts symmetrically for $Fr = 1.2$, but eventually becomes unsteady and asymmetric. An interesting feature is the flapping, i.e. lateral oscillation, that can be observed for $Fr = 1.2$ in figure 3. The flapping phenomenon can be thought of as a lateral movement of the fountain fluid on either side of the fountain source. At the extreme of each oscillation the top of the fountain is shed laterally exposing the core of the fountain. The fountain then increases in height and the process is again repeated on the other side.
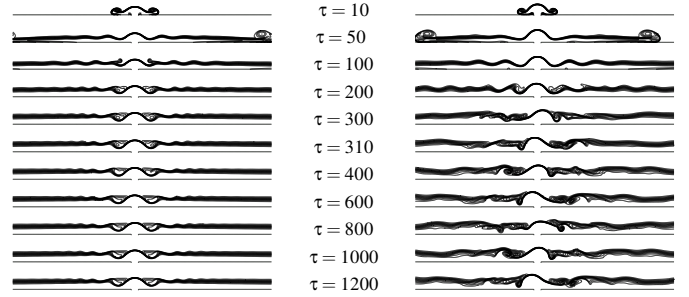

Figure 3: Evolution of temperature fields for $Fr = 1.17$ (left column) and $Fr = 1.2$ (right column) at $Re = 60$ and $Pr = 7$.

The time series of non-dimensional penetration heights for the Froude numbers $Fr = 1.17$ and $Fr = 1.2$ at $Re = 60$ and $Pr = 7$ are shown in figure 4. The fountain height in the current work is defined as the vertical distance from floor along the centre line to the location where the local temperature excess $(T - T_\infty)$ drops to 10% of the inlet excess $(T_{in} - T_\infty)$. This definition is similar to that used by Goldman and Jaluria [10] in their experiments on free-fountains. The fountain height is non-dimensionalised with half-width of the inlet manifold X_{in}. The fountain height at full development in figure 4 does not vary with time for the Froude number $Fr = 1.17$. The unsteady and periodic nature of the side to side oscillations of the flow in the flapping fountain is clearly seen in the periodic structure of the corresponding fountain height at $Fr = 1.2$, observed in figure 4.

The critical Froude number for transition at full development are mapped onto a $Re - Fr$ plot, shown in figure 5, along with the previous experimental observations of Srinarayana *et al.* [8]. The demarcation line obtained here matches very well the experimental results. The critical Froude number for unsteadiness at full development varies with the Reynolds number. For $Re \gtrsim 60$, the transition Froude number is nearly constant at $Fr \sim 1.0$; for $10 < Re \lesssim 50$, there is a steady increase in the transition Froude number; and for $Re \lesssim 10$, there is a very sharp increase in the transition Froude number. The demarcation
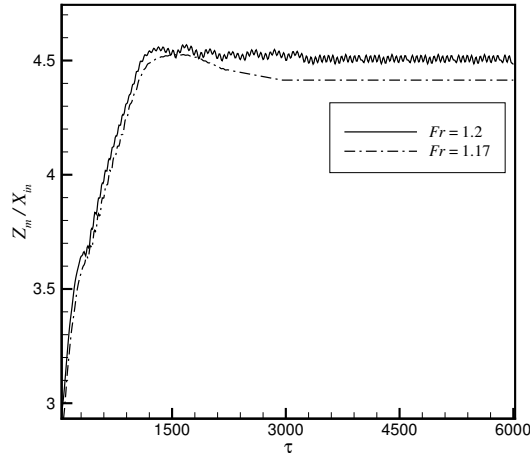
Figure 4: Time-series of non-dimensional fountain height for $Fr = 1.17$ and $Fr = 1.2$ at $Re = 60$ and $Pr = 7$.
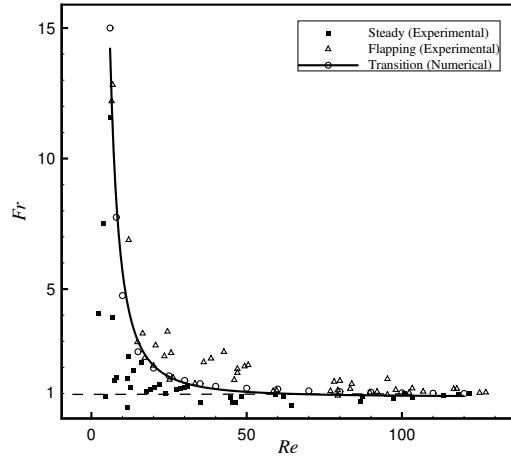

Figure 5: Re-Fr plane.

line in the present analysis is well approximated with,

$$Fr \sim 0.95 + 490\,Re^{-2} \tag{13}$$

It is however noted that Srinarayana *et al.* [8] had used three different fits to describe the fountain behaviour, that is, for $Re \gtrsim 60$ they used $Fr \sim 1.0$, for $10 < Re \lesssim 50$ the demarcation line was constant $FrRe^{-2/3}$ line, and the demarcation line for $Re \lesssim 10$ was approximated by $Fr \sim Re^{-n}$, where $n \approx 2\,\text{to}\,4$.

The critical Froude number for transition to unsteady flow obtained here for $Re \gtrsim 60$ matches well with the experimental results of Friedman *et al.* [11] for $Re \gtrsim 55$. For non-circular fountain source, their Fr was based on the inlet hydraulic diameter, $D_H = 4A_c/P_m$, where A_c is the cross-sectional area and P_m is the perimeter. For an inlet with a long span compared to the width (the present study), $D_H = 4X_o$. Based on X_o, the transition Froude number obtained by Friedman *et al.* [11] is $Fr \approx 1.0$.

Conclusions

The behavior of plane fountains at low-Reynolds number has been investigated numerically. The critical Froude number for transition from a steady to unsteady behavior at full development was mapped on to a $Re - Fr$ and was found to vary with the Reynolds number. For $Re > 60$, the critical Froude number was found to remain nearly constant at $Fr \approx 1.0$, and for lower Reynolds number $Re <= 50$ there was a significant increase in the transition Froude number. The demarcation line was well approximated by $Fr \sim 0.95 + 481Re^{-2}$. The fountain below this demarcation line were completely steady and symmetric about the fountain source at full development. The fountain above the demarcation line were unsteady and exhibits flapping behavior with repeated sideways shedding and rising of the top of the fountain. The behaviour of steady and flapping fountains was further demonstrated with the non-dimensional fountain height. The transition Froude number obtained in the present work matched well with previous experimental work and opened the way for investigation into fountain behaviour at very low Reynolds number ($Re << 5$) and into the creeping flow regime.

References

[1] B. R. Morton, Forced Plumes, J. Fluid Mech. 5 (1959) 151–163.

[2] I. H. Campbell, J. S. Turner, Fountains in magma chambers, J. Petrol. 30 (1989) 885–923.

[3] W. D. Baines, J. S. Turner, I. H. Campbell, Turbulent fountains in an open chamber, J. Fluid Mech. 212 (1990) 557–592.

[4] W. X. Lin, S. W. Armfield, Direct simulation of weak laminar plane fountains in a homogeneous fluid, Int. J. Heat Mass Transfer 43 (2000) 3013–3026.

[5] W. X. Lin, S. W. Armfield, The Reynolds and Prandtl number dependence of weak fountains, Comput. Mech. 31 (2003) 379–389.

[6] N. Srinarayana, G. D. McBain, S. W. Armfield, W. X. Lin, Height and stability of laminar plane fountains in a homogeneous fluid, Int. J. Heat Mass Transfer 51 (2008) 4717–4727.

[7] N. Williamson, N. Srinarayana, S.W. Armfield, G. McBain, W. X. Lin, Low Reynolds number fountain behaviour, J. Fluid Mech. 608 (2008) 297–317.

[8] N. Srinarayana, N. Williamson, S. W. Armfield, Wenxian Lin, Line fountain behavior at low-Reynolds number , Int. J. Heat Mass Transfer 53 (2010) 2065–2073.

[9] S. Popinet, Gerris: a tree-based adaptive solver for the incompressible Euler equations in complex geometries, J. Comput. Phys. 190 (2003) 572–600.

[10] D. Goldman, Y. Jaluria, Effect of opposing buoyancy on the flow in free and wall jets,J. Fluid Mech. 166 (1986) 41-56.

[11] P. D. Friedman, V. D. Vadakoot, W. J. Meyer Jr, S. Carey, Instability threshold of a negatively buoyant fountain, Exp. Fluid 42 (2007) 751–759.